JKAU: Eng. Sci., **Vol**.19 No.2, pp: 3-22 (2008A.D. / 1429 A.H.)

The Resistance of a Control Rolled and Aged Steel to Hydrogen Induced Cracking (HIC)

Faisal I. Iskanderani

Chemical and Materials Engineering Department,
Faculty of Engineering, King Abdulaziz University,
Jeddah, Saudi Arabia
faisalii@kau.edu.sa

Abstract. Hydrogen absorbed from environment interacts with lattice defects, precipitates and non-metallic inclusions and alters the mechanical behaviour of steel. This paper examines the role of microalloy carbide precipitate dispersions in a thermomechanically treated Ti V Nb microalloyed steel to obtain a refined grain structure for use in oil and natural gas transmission pipeslines. The positive effect of microalloy carbide precipitates of Ti, V and Nb on the resistance to hydrogen embrittlement (HE) of the steel is interpreted in terms of the hydrogen trap theory. Accordingly, hydrogen partitioned and entrapped by fine dispersions of Ti, Nb, and V carbonitride precipitates is rendered relatively harmless by causing the hydrogen concentration per trap to remain below the critical concentration level required to cause hydrogen-induced cracking (HIC). Mechanical test, scanning electron microscopy (SEM) and energy dispersive x-ray (EDAX) analytical data are presented. It is shown that appropriate thermomechanical processes designed in the light of the detailed physical metallurgy of the microalloyed steel markedly improves the hydrogen embrittlement (HE) resistance of the steel investigated. The control rolled steel aged for a short time (90 minutes) at 600^{o}C possesses excellent resistance to (HIC) and (HE) and stands as an attractive economical option for application in natural gas/oil transmission pipelines.

Keywords: Microalloyed steel, hydrogen embrittlement, control rolled steel, mechanical properties, SEM, energy dispersive x-ray.

Associate Professor, Department of Chemical & Materials Engineering, King Abdulaziz University, Ph. +966 (0)2 6952255 Fax. +966 (0)2 6952257, Email: faisalisk@gmail.com

1. Introduction

Steel pipelines designed to transport crude oil or natural gas containing traces of wet hydrogen sulphide (H_2S), a promoter of hydrogen ingress into steel are frequently reported to have developed hydrogen induced cracking (HIC), hydrogen embrittlement (HE) and hydrogen blistering (HB)[1-3]. In such circumstances where external and residual stresses are present, steel pipes may fail by either sulphide stress corrosion cracking (SSCC) due to hydrogen embrittlement (HE) or stress oriented hydrogen induced cracking (SOHIC)[2-3]. The chemical reaction that takes place between wet H_2S and the steel liberates atomic hydrogen which is readily absorbed into the steel. Diffusing hydrogen interacts with micro-structural heterogeneities in steel and gives rise to various detrimental effects.

It has long been recognized that the influence of microstructure on a given steel's susceptibility to hydrogen embrittlement can be variously critical. For instance, microstructural heterogeneities may either hasten fracture by localizing hydrogen and thus promoting a pre-existing tendency for a certain mode of failure[4]. Alternatively, heterogeneities with different characteristics can enhance the resistance to hydrogen embrittlement by uniformly partitioning hydrogen[5] and thus reducing hydrogen pressure per trap.

An investigation into the role of microstructural state on the hydrogen embrittlement of a low carbon manganese X52 steel[6] showed the susceptibility to (HE) at a given strength level to be sensitively related to the detailed microstructure, such that susceptibility to (HE) increased as the microstructure changed from ferrite-pearlite to ferrite-bainite and finally martensite. In a separate research[7] conducted on a microalloyed steel intercritically annealed and quenched to embody various proportions of martensite islands embedded in ferrite matrix, the susceptibility to (HE) of the dual-phase microstructure was shown to be greater than that of the pearlitic microstructure. The authors further noted that the residual stress arising from the austenite to martensite transformation promoted cleavage and intergranular fracture as well as (HIC) on flat surfaces.

Earlier studies by Stevens *et al*.[8] on a low carbon manganese steel microalloyed with 0.22 percent titanium quenched and tempered to yield microstructures ranging from one that contains submicroscopic TiC

precipitates to those including TiC precipitates with various degrees of coherency with the matrix clearly illustrated the effect of microstructural constituents on the resistance to (HE). Dark field transmission electron microscopy (TEM) studies[8] indicated that the microstructure consisting of a fine dispersion of semi-coherent TiC particles exhibited an outstanding resistance to (HE).

Low carbon steels microalloyed with potent carbide and nitride formers such as Ti, Nb and V and control rolled (CR) under carefully balanced thermomechanical conditions to achieve superior mechanical performance are being increasingly considered for oil/gas transportation pipelines. The thermomechanical processing, which entails simultaneous application of heat and plastic deformation to evolve a refined microstructure essentially consists of reheating the steel in the austenite phase region followed by controlled hot rolling to achieve a predetermined microstructure in the austenite prior to transformation to ferrite[9]. A number of processing parameters including steel chemistry, prior austenite grain size, rolling entry and exit temperatures, interstate rolling time interval, the strain rate per pass and the final controlled cooling (CC) rate subsequent to (CR) largely determine the final mechanical properties. It is widely concurred that the nucleation of statically recrystallized grains during the interpass time subsequent to a hot rolling pass is suppressed by the strain induced precipitates[10,11]. The ferrite grain refinement accomplished by (CR) and via the mechanism of grain growth inhibition by fine dispersions of microalloy carbides/nitrides/carbonitrides precipitating during thermomechanical processing leads to marked enhancement of yield strength and toughness.

Accelerated cooling following hot deformation is a relatively recent innovation adopted to further improve both strength and cost-effectiveness. However, very high cooling rates (20°C/S) are reported[12] to exercise a negative effect on elongation and impact toughness probably due to austenite transformation to a dual-phase microstructure composed of ferrite and martensite.

In the last decade, systematic research carried out by Alp and co-workers[13-15] has shown low carbon manganese steels microalloyed with Ti, Nb and V to develop excellent resistance to (HE) when they are subjected to an optimized thermomechanical treatment. The present work reports the effect of isothermal ageing on the resistance to (HE) of a control rolled microalloy steel.

2. Experimental Methods and Materials

2.1 Thermomechanical Processing (TMP)

The steel, procured from Sumitomo Metal Industries Ltd., Kashima Steel Works, Japan, was received in the form of 25 mm hot rolled plates and conformed to ARI 5L Grade. The detailed chemical composition of the steel microalloyed with Ti, Nb, and V is tabulated in Table 1.

Table 1. Chemical composition of the microalloy steel (weight %).

C	N	Ti	V	Nb	Mo	Ni	Cr	Mn	Cu	Si	P	S	Ca	Fe
0.04	0.035	0.015	0.04	0.043	0.01	0.017	0.02	1.28	0.27	0.21	0.06	0.04	0.03	balance

Steel slabs with the dimensions 24×150×250 mm were reheated to 1075°C and soaked for 40 minutes. Controlled rolling was carried out in accordance with the schedule described in Table 2 using a laboratory rolling mill of 40 tonne capacity.

Table 2. Controlled rolling schedule.

Roll gap setting		Thickness mm	Temperature °C	Rolling load tonne
Pass	Start	24	1075	
1	18	18.8	1050	6
2	13	13.4	1000	8
3	9	10.3	950	10.5
4	5	6.5	900	18
5	2.5	4	900	26

Clearly, in the first three passes hot rolling is accomplished in the temperature range 1075°C – 950°C which is well above the temperature at which the $\gamma \rightarrow \alpha$ transformation in this steel commences. Considering the previous estimates for the recrystallization stop temperatures[11] of steels with niobium contents similar to our steel and the effect of microalloy solutes on these temperatures[16] the present steel is reckoned to have a recrystallization stop temperature of 980°C approximately. Hence, grain refinement is thought to accrue from recrystallization that takes place during the course of the initial passes, with microalloy carbonitrides playing an increasingly inhibitive role on grain growth with progressively decreasing interpass temperatures. When the steel is deformed below its recrystallization stop temperature, an essentially cold worked grain structure results. The final cooling of the (CR) steel was carried out in air to avoid martensite formation and concomitant loss of toughness.

2.2 Post TMP Ageing Treatment

The control rolled steel was reheated to 600°C and aged at this temperature for various time intervals up to 25 hours in order to utilize the full potential of microalloy carbonitride precipitation for additional strength enhancement. Aged specimens were oil quenched to room temperature.

2.3 Mechanical Testing

Dumb-bell shaped tensile test pieces were machined from control rolled strips, with their long axis parallel to the long transverse axis of the strip. All specimens used, having a standard 20 mm gauge length, 5 mm width, and 2 mm thickness were stressed uniaxially at a cross-head speed of 2 mm/min. All flat surfaces were polished to 0.25 micron diamond finish. The mechanical behaviour of the steel in both the hydrogenated and unhydrogenated state was characterized by computer-drawn stress-strain charts.

The ageing process was monitored by conjugate hardness measurements.

2.4 Hydrogen Charging

Exquisitely polished tensile test specimens were hydrogenated in an electrochemical cell using a platinum anode, and the steel specimens as the cathode. The electrolyte, the source of H^+ ions consisted of a standard $H_2\ SO_4$ solution poisoned with a known amount of As_2O_3 to prevent H^+ ions from combining to form H_2 molecules at the cathode surface. Cathodic polarization was applied precisely 5 seconds after the specimen had been immersed in the electrolyte, using a 12-volt DC battery as a voltage supply source. A variable resistance connected in series to the circuit was employed to ensure a constant current, which was measured by a digital ammeter. The charging current, I = Current Density × exposed area of specimen surface. The constant time of hydrogenation was measured by a stop watch. Subsequent to hydrogenation the specimens were thoroughly rinsed in distilled water and then in methyl alcohol. Tensile tests were commenced consistently 5 minutes after hydrogenation to ensure identical conditions for rational comparisons.

2.5 Electron Fractography and Metallography

A scanning electron microscope operating at a maximum voltage of 30 kV and equipped with an energy dispersive x-ray (EDAX) unit was employed to study fracture surface morphology and the salient micro-structural features associated with the mode and mechanisms of fracture in both hydrogenated and unhydrogenated specimens. EDAX was extensively used for quantitative elemental analysis of both precipitates and matrix.

Flat surfaces of steel specimens in the control rolled state, and following ageing were etched in 2 percent nital solution to reveal the detailed microstructure and to identify microstructural constituents at grain boundaries and within individual grains.

3. Discussion of Results

3.1 Mechanical Properties of Control Rolled Steel

The mechanical behaviour of the control rolled steel is characterized by the nominal stress-strain curve presented in Fig. 1. The steel exhibits clear yielding at a stress level of 435 MPa. Necking occurs around 502 MPa at a total strain of 15 percent. A tensile ductility of 30 percent is noted.

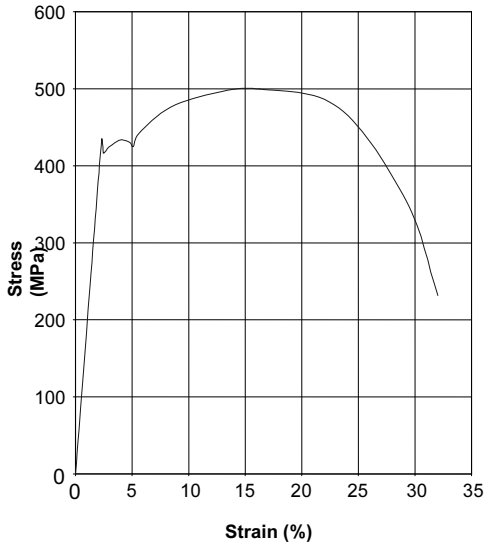

Fig. 1. Stress-strain curve of the control rolled steel.

A given set of mechanical properties imparted to a steel by thermomechanical processing would result from various reinforcing or conflicting micromechanisms and physical processes that operate during controlled rolling. Among the various strengthening mechanisms ferrite grain refinement is identified as the most significant method to enhance the yield strength and impact resistance[17-22]. In order to maximize ferrite grain refinement from austenite transformation, it is imperative to maximize the rate of ferrite nucleation and minimize the rate of grain growth and subsequent coarsening. To achieve this objective, the number of nucleation sites, that is the total austenite grain boundary area, per unit volume, including sub-grain surfaces, deformation bands and twin boundaries, and the nucleation frequency per site need to be maximized at the threshold of austenite-to-ferrite transformation.

Figure 2 depicts the microstructure of the steel following controlled rolling. With an average grains size of around 8 microns grain refinement is evident. Due to the last three passes being carried out below the recrystalization stop temperature grains appear to be somewhat flattened in the rolling plane (Fig. 3). Grain boundary and intra-grain precipitation of largely submicron size microalloy nitrides and carbides is barely observable. TiN and NbC were more frequently encountered than other species.

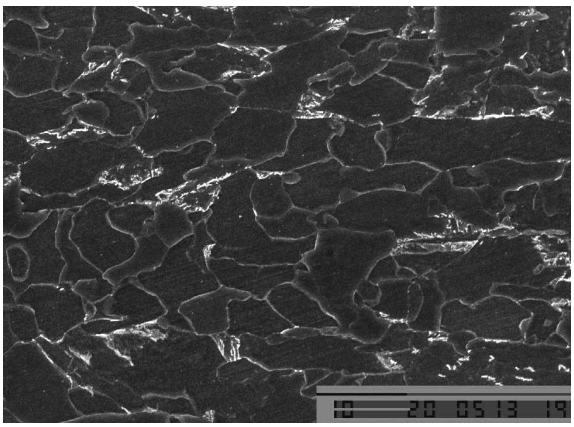

Fig. 2. Microstrucure of CR steel compising refined grains with microalloy nitrides and carbides at grain boundaries.

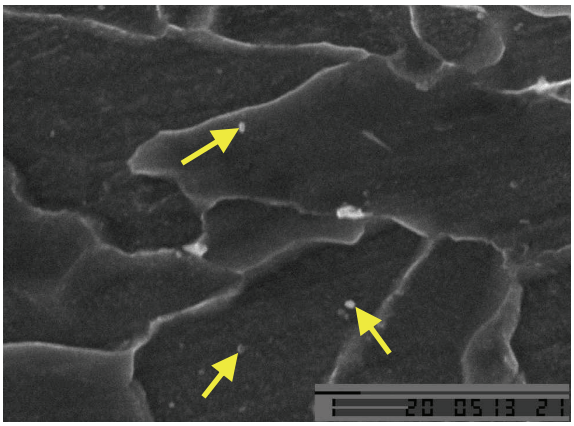

Fig. 3. Grains somewhat elongated during rolling below the recrystallization stop temperature of the steel.

3.2 The Mechanical Behaviour of the Steel Control Rolled and Aged at 600°C.

The ageing process was first followed by hardness measurements which indicated a steep rise in hardness within the first 60 minutes. Maximum hardness was attained in 90 minutes, registering a 40 percent increase over that recorded just before the start of ageing (Fig. 4). Prolonged ageing beyond 90 minutes resulted in a similarly sharp fall within a time span of approximately 60 minutes. Henceforth, hardness continued to decline at a much less conspicuous rate. Following 24 hours of ageing, the hardness level was about 5 percent less than it was at the outset of ageing.

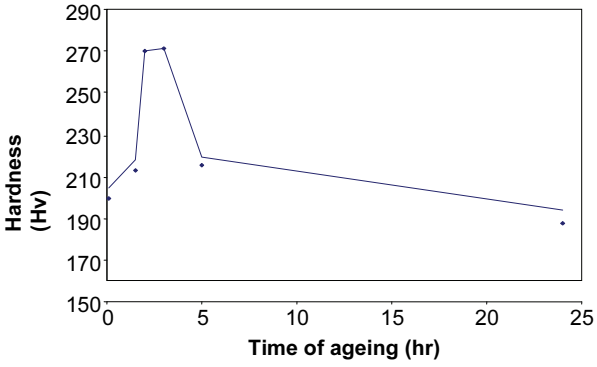

Fig. 4. hardness *vs.* ageing time at 600°C.

The two phenomena of precipitation strengthening and precipitate coarsening are well known and need not be discussed here in detail. Suffice it to say that the increase in hardness in the initial stage of ageing is unequivocally related to the formation of fine dispersions of precipitates fully or partially coherent with the matrix. These precipitates effectively impede dislocation glide thereby raising the strength. Whilst, the decrease in hardness is associated with coarsening of precipitates, which become incoherent with the matrix as they grow and strain incompatibility develops across the precipitate/matrix interfaces.

The microstructure of the steel following 90 minutes of ageing at 600°C comprises a ferritic matrix with microalloy carbide/nitride particles presiding at dislocations, grain boundaries, sub-boundaries and deformation bands (Fig. 5). The submicron size particles with only few micron inter-particle spacing give rise to marked increase of 19 percent in the yield strength (516 MPa), and 15 percent increase in the UTS (575 MPa) (Fig. 6). The breaking strength (BS) similarly increases by 20 percent to around 280 MPa. As the stress-strain curve in Fig. 6 indicates, a tensile ductility of 30 percent is maintained. Hence, as SEM observations of the fracture surface reveal, a ductile mode of fracture is evidenced by extensive dimpling and microvoid coalescence (Fig. 7).

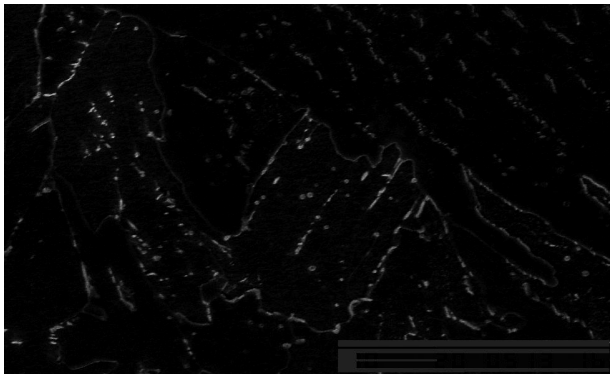

Fig. 5. Microalloy carbonitride precipitation in CR steel aged at 600°C for 90 minutes (nital etch).

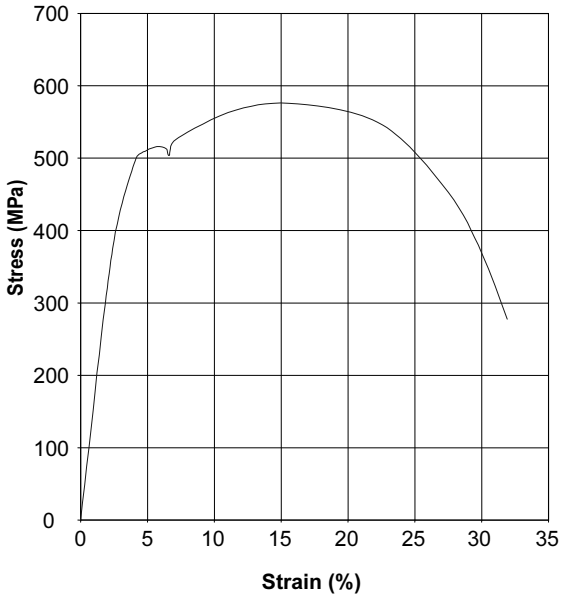

Fig. 6. The stress-strain curve of steel aged at 600°C for 90 minutes.

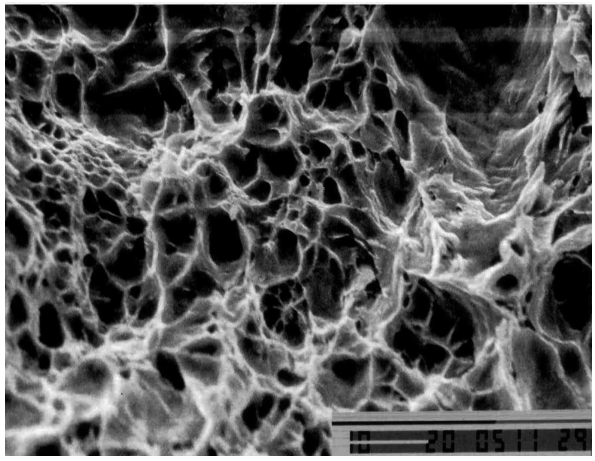

Fig. 7. Dimpled fracture surface in steel CR, and aged at 600°C for 90 minutes.

Ageing the steel at 600°C for 24 hours decreases the strength considerably (Fig. 8). The yield strength falls to 460 MPa, while the UTS and BS decline to 505 MPa and 245 MPa respectively. Elongation at fracture experiences a negligible decrease to 29 percent. The decrease in

strength is attributed to precipitate coarsening when microalloy precipitates grow in size but decrease in number density, thus being rendered less effective obstacles to dislocation movement (Fig. 9).

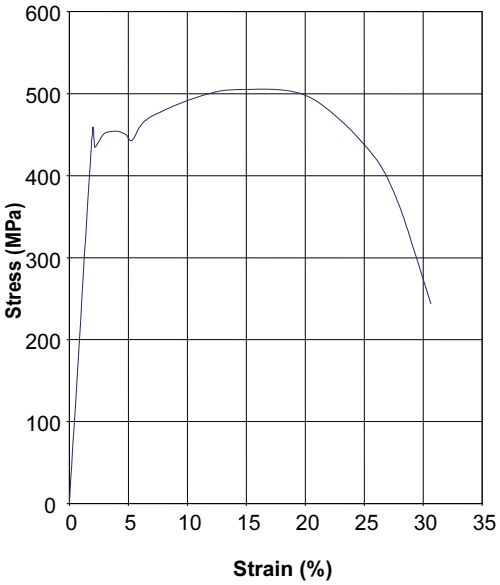

Fig. 8. Stress-strain curve of CR steel following ageing at 600°C for 24 hours.

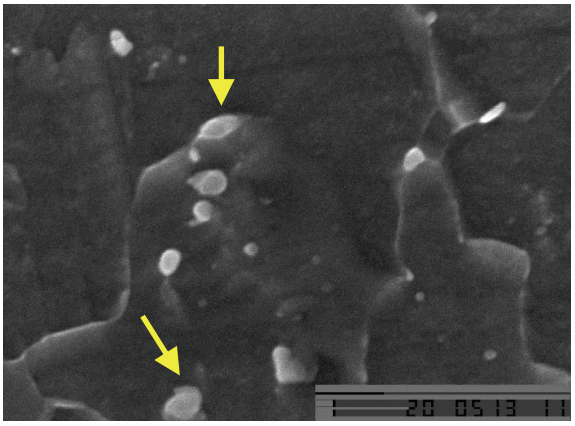

Fig. 9. Coarsened precipitates in the steel overaged (24 hours) at 600°C.

The mode of fracture in the overaged steel is evidently ductile (Fig. 10a). The fracture surface is characterized by a honeycomb structure and micro-void coalescence. Decohesioned microalloy precipitates are

frequently encountered features in the fracture surface. EDAX analysis (Fig. 10b) confirmed, these particles, approximately 5 Micron in diameter, to be VN, NbN and TiN, in order of descending frequency.

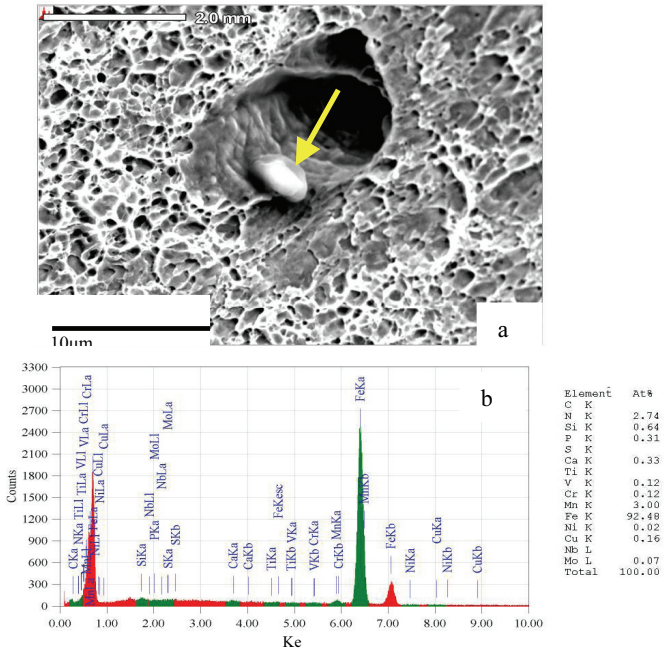

Fig. 10. a. Ductile mode of fracture in steel overaged 24 hours at 600°C.
b. EDAX analysis of a microalloy recipitate (arrowed).

3.3 The Effect of Hydrogen on Mechanical Properties

The stress-strain curve of the CR steel charged with hydrogen is presented in Fig. 11. The charged yield strength (~460 MPa), UTS (509 MPa) and BS (300 MPa) all experience increments, the greatest contributions being assigned to the BS and yield stress respectively. The increase in the yield strength may be interpreted in terms of hydrogen-dislocations interaction which may arise from formation of a "hydrogen atmosphere" around mobile dislocations. Accordingly, it is, assumed that a fraction of the hydrogen is partitioned between and trapped by microalloy precipitates innocuously by virtue of whose fine dispersion the hydrogen concentration is maintained below the critical level required to initiate hydrogen induced cracking (HIC). During the course of plastic deformation, the hydrogen dissolved in the ferrite lattice is swept by and progressively accumulated around mobile dislocations.

Thus, the resistance to dislocation glide continues to build up resulting in enhanced yield strength compared to that of the unaged CR steel. This trend continues as long as the increase in the population of sufficiently fine precipitates in the context of homogeneous distribution of hydrogen, with ageing persists. Thus as Fig. 12 clearly manifests the charged yield strength in the steel aged for a short interval (90 minutes) to yield fine dispersion of microalloy precipitates, (482 MPa) is superior to that of the unaged steel in the charged states (460 MPa). By the same token, the charged yield strength of the steel aged for 24 hours is unambiguously incrased to 500 MPa (Fig. 13).

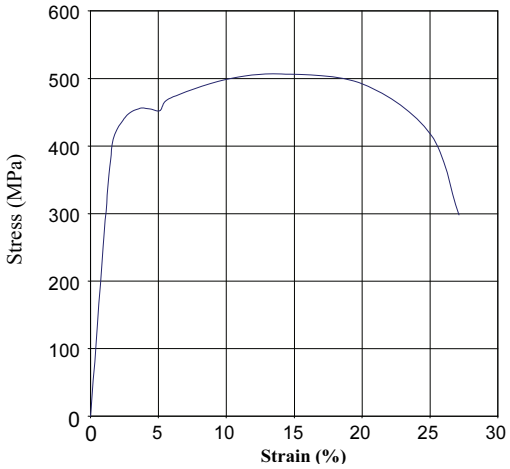

Fig. 11. Stress-strain curve of hydrogenated CR steel.

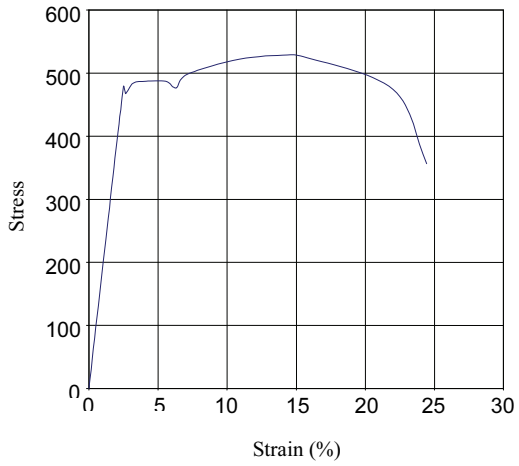

Fig. 12. The charged stress-strain curve of the CR steel aged at 600°C for 90 minutes.

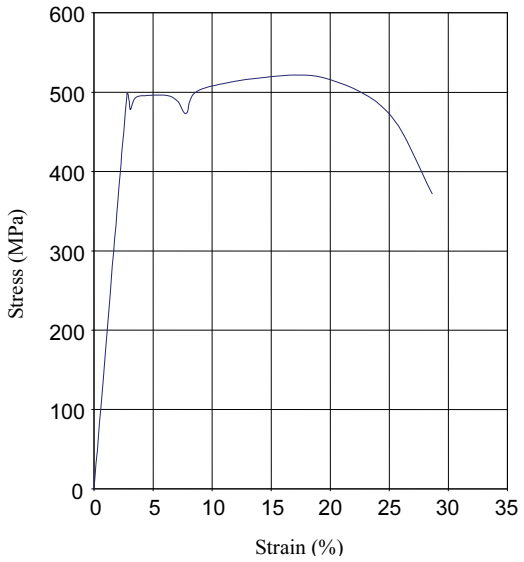

Fig 13. The charged stress-strain curve for the steel aged at 600°C for 24 hours.

The increase in the charged UTS (~530 MPa) relative to the UTS of the uncharged CR steel (502 MPa) registered upon ageing for 90 minutes may be accounted for in terms of increased matrix strain leading to enhanced work hardening engendered by interaction of dislocations restricted in slip by the hydrogen atmosphere surrounding them. Nevertheless, with prolonged ageing (24 hours) causing relative coarsening of microalloy precipitates, the charged UTS exhibits a modest fall to 520 MPa (Fig. 13). Figure 14 compares the variation of the charged and uncharged UTS with ageing time. The deleterious influence of hydrogen on the peak strength corresponding to 90 minutes ageing is evident. The uncharged UTS is reduced considerably from 575 MPa to 530 MPa. Nevertheless, with increasing ageing time the strength gap is bridged so that at 18 hour ageing, at the intersection of the two curves the charged and uncharged strengths become identical (~523 MPa). Henceforth, while the uncharged UTS continues to diminish, the charged UTS is maintained at 520 MPa approximately.

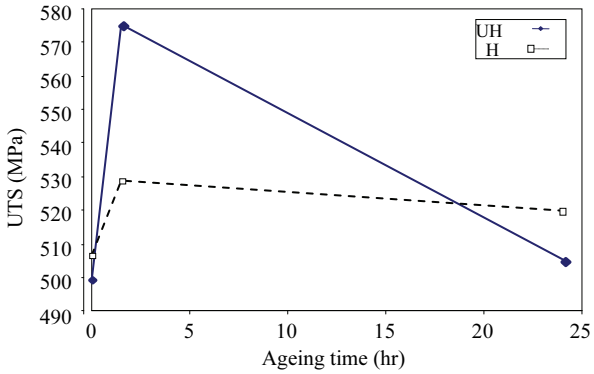

Fig. 14. The UTS *vs.* ageing time at 600°C for hydrogenated (H) and un-hydrogenated (UH) steel.

Figure 15 compares the uncharged and charged tensile ductilities of the steel over an ageing period of 24 hours. As pointed out previously elongation at fracture of the CR steel indicates a negligible change from 30 percent to 29 percent after 24 hour ageing, and the fracture surface bears all the characteristics as a ductile mode of failure (Fig. 16). However, hydrogenation causes the elongation of the CR steel to decrease to 26 percent. A measurable decrease in elongation occurs following hydrogenation of the steel aged for 90 minutes, when the tensile ductility falls from 28 percent for the CR steel to around 26 percent for the steel aged for 90 minutes. This slight decrease may be related partly to the interaction of hydrogen with the coherency strains across the precipitate/matrix interfaces. The lowest charged elongation (~23%) is observed, in the steel aged for 24 hours. At this stage, although (HIC) initiated at non-metallic inclusions is observed (Fig. 17), the mode of fracture remains predominantly ductile (Fig. 18).

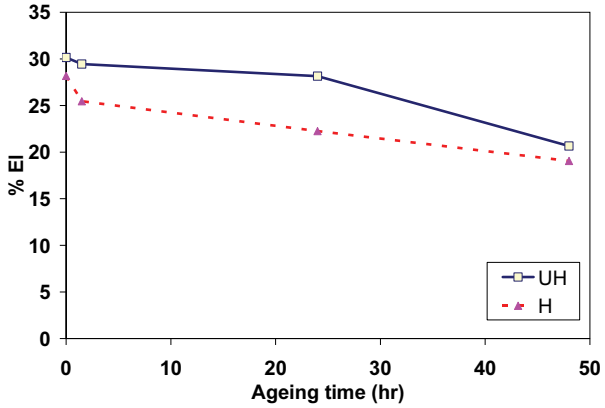

Fig. 15. Charged and uncharged elongation vs ageing time at 600°C.

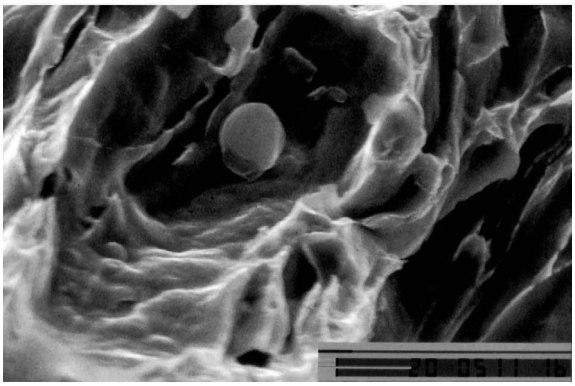

Fig. 16. Ductile mode of fracture in steel aged at 600°C for 24 hours. A decohesioned microalloy precipitate rests against a ductile ferritic matrix.

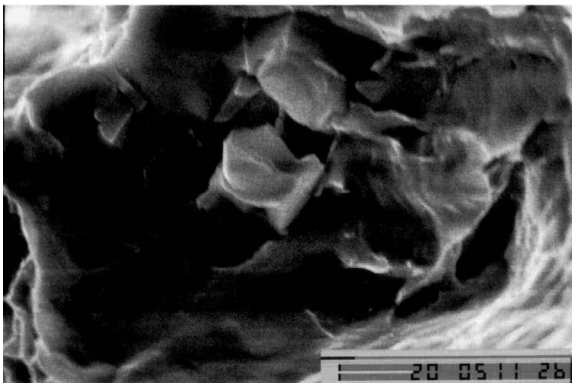

Fig. 17. An aggregate of non metallic inclusions associated with (HIC).

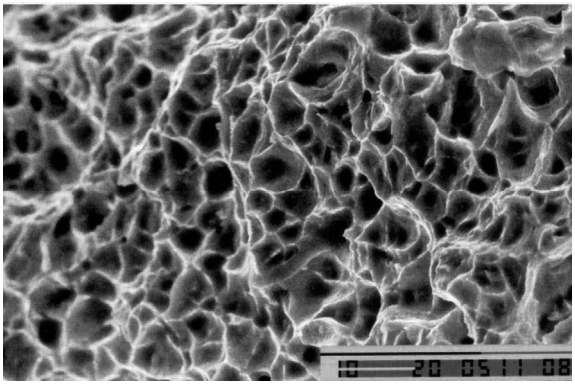

Fig. 18. The ductile matrix surrounding the (HIC) location seen in Fig 17.

4. Conclusions

i. The steel control rolled to obtain a refined grain structure and fine dispersions of microalloy carbonitride precipitates of Ti, Nb and V, exhibits a superior resistance to hydrogen embrittlement.

ii. Short-term charging of the CR steel with hydrogen increases the strength appreciably. This is ascribed to hydrogen atmospheres interfering with dislocation movement.

iii. The CR steel manifests precipitation strengthening when aged at 600 ^{o}C for about 90 minutes.

iv. The hydrogenated ductility of the precipitation strengthened steel is excellent and comparable to that of hydrogenated CR steel.

v. Overageing in the interval 2-24 hours results in loss of strength due to relative precipitate coarsening.

vi. The CR steel aged for a short time (90 minutes) exhibits an optimum combination of charged strength (530 MPa) and tensile ductility (26%), and provides an attractive economic option for the natural gas/oil pipeline design.

References

[1] **Rogante, M., Battistella, P.** and **Cesari, F.,** Hydrogen Interaction and Stress Corrosion Cracking in Hydrocarbon Storage Vessel and Pipeline Weldings, *International Journal of Hydrogen Energy*, **31**: 597-601(2006).

[2] **Azevedo, C.R.F.,** Failure analysis of a crude oil pipeline, *Engineering Failure Analysis*, **14**(6): 978-994 (2007).

[3] **Carneiro, R.A., Ratnapuli, R.C.** and **Lins, V.F.C.**, The influence of chemical composition and microstructure of API linepipe steels on hydrogen induced cracking and sulfide stress corrosion cracking, *Mater. Sci. and Eng*., **A357**: 104-110 (2003).

[4] **Bernstein, I.M.** and **Thompson, A.W.**, Selection of structural materials for hydrogen pipelines and storage vessels, *International Journal of Hydrogen Energy*, **2**(2): 163-173 (1977).

[5] **Pressuyre, G.M.** and **Bernstein, I.M.,** An example of the effect of hydrogen trapping on hydrogen embrittlement, *Metall. Trans*., **12**(5): 835-844 (1981).

[6] **Alp, T., Davies, T.J.** and **Dogan, B.**, Effect of microstructure in the hydrogen embrittlement of a gas pipeline steel, *J. Mater. Sci.*, **22**: 2105-2112 (1987).

[7] **Alp, T., Iskanderani, F.I.** and **Zahed, A.H.**, Hydrogen effects in a dual-phase microalloy steel, *J. Mater. Sci*., **26**: 5644-5654 (1991).

[8] **Stevens, M.F., McInteer, W.A.** and **Bernstein, I.M.**, *3rd. Int. Conf. Effects of Hydrogen on Behaviour of Materials*, (ed.) A.W. Thompson and I.M. Bernstein, AIME, Warrendale, P.A., (1981).

[9] **DeArdo, A.J.**, Understanding Microstructure: Key to Advances in Materials, *Conf. Proc. of Int. Metallographic Soc., Microstructural Science*, Vol. **24**, Pittsburg, 1996, (ed.) M.G. Burke, E.A. Clark and E.J. Palmiere, p. 51.

[10] **Kwon, O.** and **DeArdo, A.J.**, Interactions between recrystallization and precipitation in hot-deformed microalloyed steels, *Acta Met*., **39**: 529 (1991).
[11] **Palmiere, E.J., Garcia, C.I.** and **DeArdo, A.J.**, The Influence of Niobium Supersaturation in Austenite on the Static Recrystallization Behavior of Low Carbon Microalloyed Steels. *Metall. Trans*, **27**: 951-960 (1994).
[12] **Bakkaloglu, A.**, Effect of processing parameters on the microstructure and properties of an Nb microalloyed steel, *Materials Letters*, **56**(10): 200-209 (2002).
[13] **Alp, T.** and **Iskanderani, F.I.,** "*Development of Steel for the Oil and Gas Industries*", Final Report, Funded Research, KAU, Jeddah (1991).
[14] **Alp, T., Iskanderani, F.I.** and **Zahed, A.H.**, "Hydrogen Embrittlement of X52 and X70 Microalloy Steels", *Proc. 4th Saudi Eng. Conf., Dhahran*, Vol. **5**, p. 159 (1995).
[15] **Alp, T., Iskanderani, F.I.** and **Zahed, A.H.**, "*The Effect of Microalloy Precipitates on the Hydrogen Embrittlement of a Natural Gas/Oil Pipeline Steel*", Final Report, Funded Research, KAU, Jeddah (1997).
[16] **Cuddy, L.J.,** *Plastic Deformation of Metals*, Academic Press, New York, pp: 129-140. (1975).
[17] **Hall, E.O.**, The Deformation and Ageing of Mild Steel: III Discussion of Results, *Proc. Physical Soc.,* **Series B**, 64B, 747 (1951).
[18] **Wesbster, D.** and **Woodhead, J.A.,** Effect of 0.03% Nb on the Ferrite, Grain Size of Mild Steels, *J. Iron Steel Inst*., **202**: 987 (1964).
[19] **Morrison, W.B.** and **Chapman, J.A.,** "Controlled rolling," *Symp. Metals Soc. National Physical Lab. and Royal Soc., London (1976),* pp: 286-303, Phil. Trans. Roy. Soc., 282, 289(1976).
[20] **Pickering, F.B.**, *Proc. Microalloying* 75 (Washington, DC), Union Carbide Corp., New York, p. 9 (1977).
[21] **Zajac, S., Siwecki, T.** and **Hutchinson, B.**, Recrystallization controlled rolling and accelerated cooling for high strength and toughness in V-Ti-N steels, *Metall. Trans*., **22**(11): 2681-2694 (1991).
[22] **Siwecki, T., Hutchinson, B.** and **Zajac, S.,** Microalloying 95, *Proc. Int. Conf. on Microalloying, Pittsburg, PA*, p. 197 (1995).

مقاومة صلب مدلفن بتحكم ومعتق للتصدع المستحث بالهيدروجين

فيصل إبراهيم إسكندراني

قسم الهندسة الكيميائية وهندسة المواد، كلية الهندسة، جامعة الملك عبد العزيز

جدة – المملكة العربية السعودية

faisalii@kau.edu.sa

المستخلص. يقوم الهيدروجين الممتص من الجو بتغيير السلوك الميكانيكي للصلب، وذلك بتفاعله مع الشوائب الموجودة في تركيبه الصلب، وكذلك مع الرواسب والمحتويات غير المعدنية. يقدم هذا البحث دراسة عن ترسبات سبيكة الكربايد المتناثرة في سبيكة صلب (تيتانيوم، وفناديوم، ونيوبيوم) معالجة بطريقة حرارية ميكانيكية، حيث تؤدي إلى تكون بنية دقيقة للصلب تجعل استخدامه مناسبًا لصناعة أنابيب نقل النفط والغاز الطبيعي.

يمكن تفسير هذا التأثير الإيجابي لترسبات سبيكة الكربايد المتناثرة على سبيكة صلب (تيتانيوم، وفناديوم، ونيوبيوم) بنظرية مصائد الهيدروجين. وبالتالي فإن الهيدروجين المجزأ والمحسن بواسطة ترسبات سبيكة الكربونايترايد (تيتانيوم، وفناديوم، ونيوبيوم) يقل تأثيره كثيرًا، لأن تركيزه في كل مصيدة يصبح أقل من الحد الحرج المسبب للتصدع.

تم عرض نتائج الاختبار الميكانيكي والمسح المجهري الإلكتروني والطاقة والأشعة السينية متبددة الطاقة (إداكس). واستنتج أنه يمكن تحسين مقاومة الصلب (المستخدم في هذا البحث) لتقصيف الهيدروجين بدرجة ملحوظة، إذا ما تم تصميم عمليات

حرارية ميكانيكية ملائمة، بناءً على الـصفات المعدنيـة لـسبيكة الصلب. إن الصلب المدلفن بتحكم في ٩٠ دقيقة عند درجة حرارة ٦٠٠ درجة مئوية يمتلك مقاومة ممتازة لتقصيف الهيدروجين، مما يجعله خيارًا اقتصاديًا جذابًا للاستخدام في صناعة أنابيب نقل النفط والغاز الطبيعي.